THE ANATOMICAL RECORD 293:1192–1206 (2010)

Muscle Architecture in the Mystacial Pad of the Rat

SEBASTIAN HAIDARLIU,[1]* EREZ SIMONY,[1] DAVID GOLOMB,[2] AND EHUD AHISSAR[1]

[1]Department of Neurobiology, The Weizmann Institute of Science, Rehovot, Israel
[2]Department of Physiology, Zlotowski Center for Neuroscience, Ben-Gurion University of the Negev, Beer-Sheva, Israel

ABSTRACT

The vibrissal system of the rat is an example of active tactile sensing, and has recently been used as a prototype in construction of touch-oriented robots. Active vibrissal exploration and touch are enabled and controlled by musculature of the mystacial pad. So far, knowledge about motor control of the rat vibrissal system has been extracted from what is known about the vibrissal systems of other species, mainly mice and hamsters, since a detailed description of the musculature of the rat mystacial pad was lacking. In the present work, the musculature of the rat mystacial pad was revealed by slicing the mystacial pad in four different planes, staining of mystacial pad slices for cytochrome oxidase, and tracking spatial organization of mystacial pad muscles in consecutive slices. We found that the rat mystacial pad contains four superficial extrinsic muscles and five parts of the *M. nasolabialis profundus*. The connection scheme of the three parts of the *M. nasolabialis profundus* is described here for the first time. These muscles are inserted into the plate of the mystacial pad, and thus, their contraction causes whisker retraction. All the muscles of the rat mystacial pad contained three types of skeletal striated fibers (red, white, and intermediate). Although the entire rat mystacial pad usually functions as unity, our data revealed its structural segmentation into nasal and maxillary subdivisions. The mechanisms of whisking in the rat, and hypotheses concerning biomechanical interactions during whisking, are discussed with respect to the muscle architecture of the rat mystacial pad. Anat Rec, 293:1192–1206, 2010. © 2010 Wiley-Liss, Inc.

Key words: consecutive tissue slices; histochemical staining; muscle architecture; rat mystacial pad; rodent whisking mechanisms

Grant sponsor: European Commision grant; Grant number: BIOTACT (ICT-215910); Grant sponsor: The Minerva Foundation funded by the Federal German Ministry for Education and Research; Grant sponsor: United States–Israel Binational Science Foundation; Grant number: 2007121; Grant sponsor: The Phyllis and Joseph Gurwin Fund for Scientific Advancement; Grant sponsor: The Israel Science Foundation; Grant number: 95906; Grant sponsor: The Nella and Leon Benoziyo Center for Neurological Diseases.

*Correspondence to: Sebastian Haidarliu, Department of Neurobiology, The Weizmann Institute of Science, Rehovot 76100, Israel. Fax: 972-8-9346099.
E-mail: sebastian.haidarliu@weizmann.ac.il

Received 17 September 2009; Accepted 14 February 2010
DOI 10.1002/ar.21156
Published online 13 April 2010 in Wiley InterScience (www.interscience.wiley.com).

Mystacial pads on the snouts of rodents contain motor-sensory plants that are controlled via the facial nerve and drive the trigeminal nerve. Each pad is a complex structure that contains about 35 large vibrissae (whiskers) that are used for active touch via whisking. The muscles of the mystacial pad are considered to be the primary movers of the vibrissae during whisking.

In rodents, muscles of the mystacial pad are part of superficial facial group of muscles, and can be referred to as orbitonasal musculature (Rinker, 1954; Klingener, 1964; Ryan, 1989). In whisking rodents, all the muscles of the mystacial pad can be divided into two categories: extrinsic muscles that originate on the skull and/or nasal cartilage and insert into mystacial pad from different directions, and intrinsic muscles that are associated with vibrissal follicles and partially with the corium, and are not directly attached to the skull. Specific organization of the musculature in the mystacial pad for some individual species of whisking rodents [mice (Dorfl, 1982), and hamsters (Wineski, 1985)] has been described in detail. Since a similar detailed description of the anatomy of the mystacial pad in rats was lacking, most studies involving the rat mystacial pad (White and Vaughan, 1991; Berg and Kleinfeld, 2003; Guntinas-Lichius et al., 2005; Nguyen and Kleinfeld, 2005; Shaw and Liao, 2005; Angelov et al., 2007; Hill et al., 2008) utilized extrapolations from descriptions of the extrinsic and intrinsic muscle organization proposed specifically for mice and hamsters. However, such extrapolation is not reliable because of differences between rodent species, including mice and hamsters, with regard to mystacial pad musculature, and probably between the rat and other rodent species. For example, in mice, only four extrinsic muscles were assigned to the mystacial pad (Dorfl, 1982), whereas, in the hamster, seven extrinsic muscles have been assigned (Wineski, 1985). One of these extrinsic muscles, the *M. nasolabialis profundus*, is composed of five distinct parts, of which three are directly associated with vibrissae. An analog of the *M. nasalis* described in mice (Dorfl, 1982) has not been found in hamsters (Wineski, 1985). Similarly, three parts of the *M. nasolabialis profundus*, which have insertion sites in the mystacial pad of hamsters (Wineski, 1985), have not been detected in mice (Dorfl, 1982). Such differences between two extensively-studied species of whisking rodents support interspecies differences in mystacial pad architecture, and were the stimuli for launching our study of the rat mystacial pad muscle architecture to further understand the role of mystacial pad muscles in the whisking behavior of rats.

Although intrinsic muscles of the rat mystacial pad were observed in the 19th century, detailed descriptions, such as their being flat muscles that surround vibrissal follicles on three sides (Vincent, 1912), and that a group of small follicular muscles associate only with vibrissa follicles (Dorfl, 1982), were recorded much later. In the hamster, intrinsic muscles of the mystacial pad were described as vibrissal capsular muscles with the same appearance and distribution as in mice (Wineski, 1985). These intrinsic mystacial pad muscles are sometimes referred to as "capsular" or "sinus hair" muscles. Intrinsic muscles are considered to be the muscles that cause whisker protraction.

Construction of a biologically-inspired, robotic implementation of the rat whisker sensory system was recently attempted (Pearson et al., 2007; Mitchinson et al., 2008). Reliable bio-mimicry requires a detailed knowledge of the morphology and mechanics of the vibrissae and muscles within the mystacial pad of the rat. The hypothesis guiding this research is that active whisking and touch are manipulated by a complex combination of multiple muscle systems within the mystacial pad. Exactly how each muscle contributes to specific aspects of whisking and touch depends critically on the anatomical arrangement of these muscles in relation to the whisker follicles and surrounding tissue. In this study, we describe the musculature of the entire Wistar rat mystacial pad, especially the origin and insertion sites for each muscle, so that the precise spatial arrangement of the muscles can be determined, which could then be used to construct biomechanical models of the rat mystacial pad. Comparison of the anatomical characteristics of the rat mystacial pad muscles with mystacial pad musculature previously described in mice and hamsters was achieved by cutting rat mystacial pads in different planes, and staining consecutive slices of the mystacial pad for cytochrome c oxidase (CCO) activity. Our assessment relied heavily on topographic features, such as origin and insertion, and position relative to the other facial muscles or vibrissae in *in situ* conditions. The reconstruction, based on our results, of the anatomical organization of the musculature in the rat mystacial pad, confirmed a general correspondence of the majority of rat mystacial pad muscles to the ones in mice and hamsters, with several peculiar differences. These differences refer to a group of deep extrinsic muscles that are synergistic to the intrinsic muscles, but can also control the degree of whisker spread.

MATERIALS AND METHODS

Animals

The snout musculature of 25 male albino Wistar rats of various ages (four 2 to 3-week-old, seventeen 4-month-old, and four 1-year-old) was examined. Organization of the rat mystacial pad was also studied in 10–14-day-old rat embryos. The procedures for animal maintenance and all manipulations were approved by the Institute's Animal Care and Use Committee, and conform to the NIH Principles of Laboratory Animal Care (publication No. 86-23, revised 1985). Rats were anesthetized intraperitoneally with urethane (25%; 0.65 mL/100 g body weight), perfused transcardially (2.5% glutaraldehyde, 0.5% paraformaldehyde, and 5% sucrose in 0.1 M phosphate buffer, pH 7.4), and then decapitated. Musculature of the mystacial pad was visualized by light microscopy of serial sections histochemically stained for CCO activity.

Staining for CCO Activity

After perfusion, the rostral region of the muzzle was removed, cut along the sagittal plane into two symmetric halves, and postfixed in the solution used for perfusion, to which additional (25%) sucrose was added. In adult rats, after the first 24 hr of postfixation, the nasal bones and premaxilla were removed from the muzzle tissue, and the mystacial pads were placed between two pieces of stainless steel grid in a slightly flattened status in RCH44 perforated plastic histology cassettes (Proscitech.com) to

prevent curling of the mystacial pad during dehydration. The cassettes were then placed into the same postfixation solution for another 24 hr. The mystacial pads of 2- and 3-week-old rats were postfixed *in situ* for 48 hr.

After postfixation, each mystacial pad was sectioned with a sliding microtome (SM 2000R; Leica Instruments, Germany) coupled with a freezing unit (K400; Micron International, Germany) into 60 μm thick sections in one of four planes: horizontal, tangential (parasagittal), coronal, and oblique (vertically, ~45 degrees to the sagittal plane). All slices were stained for CCO activity according to our modification (Haidarliu and Ahissar, 2001) of a procedure by Wong-Riley (1979). Briefly, free-floating slices were incubated in oxygenated solution of 4% sucrose, 0.02% cytochrome c (Sigma), catalase (200 μg/mL), and 0.05% diaminobenzidine in 0.1 M phosphate buffer for 2–3 hr at room temperature under constant agitation. When clear differentiation between highly reactive and non-reactive tissue structures is achieved, the incubation is arrested by rinsing with 0.1 M phosphate buffer. Stained slices were coverslipped with Entellan, and subjected to light microscopy.

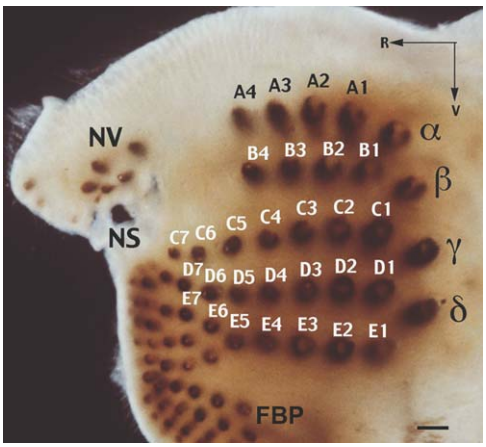

Fig. 1. Spatial organization of the mystacial vibrissae of the rat. Blood sinuses that surround whisker roots were visualized using xylene (Haidarliu and Ahissar, 1997). α–δ, the four caudal-most vibrissa follicles (straddlers); **A**–**E**, the five vibrissal rows; FBP, furry buccal pad; NS, nostril; NV, nasal vibrissae; R, rostral; V, ventral; scale bar = 1 mm.

Preparation of Figures

All figures were prepared from digital images. An Axiolab microscope (Zeiss), or a Nikon fluorescent microscope (Nikon Eclipse 50i), equipped with low magnification objectives 2.5× or 1.25 and 2× or 1, respectively, were used to obtain bright-field images that were imported into Adobe Photoshop software (version CS) for preparation of figures. Only minimal adjustments in the contrast and brightness of the figures were made.

RESULTS

Vibrissa and Muscle Arrangement within the Rat Mystacial Pad

In the rat, mystacial vibrissae form a symmetric tactile sensory array on both sides of the snout. Vibrissae are long thick hairs that originate from large follicles with strong capsules and blood-containing sinuses. Visualization of these sinuses revealed the spatial organization of vibrissa follicles in entire mystacial pad preparations (Fig. 1). The typical architecture of mystacial vibrissae in rats includes four straddlers (α–δ) and five rows (A–E) of vibrissae. Each row contains from 4 to 7 vibrissae that are arranged in arcs. Whisker movements are generated by a set of muscles inserted into mystacial pad. These muscles were visualized for mapping by staining for CCO activity. This staining method preserves tissue architecture, prevents excessive tissue shrinkage and deformation, and selectively stains muscle cells proportionally to their CCO activity.

We found that the arrangement of facial musculature in the rat follows general organizational principles for mammals, as described by Huber (1930a,b). Histochemical staining for CCO activity clearly revealed muscles present in the mystacial pad and which are involved in vibrissal movement. All the extrinsic muscles of the rat mystacial pad displayed a spatially divergent pattern: their insertion field was always larger than their site of origin, and the direction of the lateral portions of the muscle fibers was away from the axial portion of the muscle. Thus, contraction of different portions of such muscles should result in a movement of the whisker pad compartments that changes the position of a part of whiskers relative to the other whiskers, and consequently, probably causes a rotation of the entire whisker pad.

We observed that some of the superficial and deep muscles are only inserted into the dorsal part of the mystacial pad represented by rows A and B, while the others are inserted only into the ventral part represented by rows C–E. We refer to these compartments as *nasal* and *maxillary* subdivisions of the mystacial pad, respectively. Such compartmentalization occurs during embryonic development and was described in other rodent species (Yamakado and Yohro, 1979).

Most of the proximal ends of the vibrissal follicles end within the plate. In some mystacial slices, these ends appeared to extend beyond the plate, appearing to only be feebly attached to the plate. In fact, in tangential slices, empty holes, through which the inner ends of the follicles protruded into the subcapsular zone, were seen in the plate. During whisker protraction, the proximal ends of the vibrissal follicles can protrude deeper, which would prevent excessive extension of the corium by the distal ends of the follicles.

Defining Characteristics of Various Muscles of the Rat Mystacial Pad

Extrinsic muscles. During evolution of rodents, specialized head elements, such as the muscles that control movement of vibrissae, have been derived from the *M. platysma myoides* and *M. sphincter colli profundus* (Huber, 1930a,b). Muscles related to the mystacial pad of rodents have been described as belonging to the superficial facial muscle group (Rinker, 1954; Klingener, 1964). However, different authors used different names to describe these muscles. Recently, Diogo et al. (2009) proposed a unifying nomenclature for the facial muscles of the Mammalia as a whole. For the majority of mystacial muscles, herein, we utilized terminology that conforms to the *Terminologia Anatomica* (1998), a revision of *Nomina Anatomica*, with corresponding English

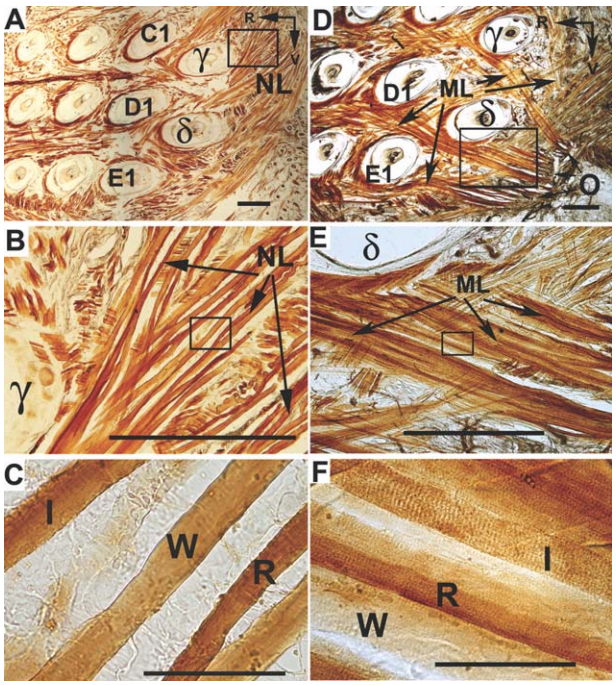

Fig. 2. Corium whisker retractors of the rat mystacial pad. (**A,D**) Superficial tangential slices of the mystacial pad from an adult Wistar rat. Slices were stained for CCO activity. (**B,E**) Higher magnification of boxed areas in (**A**) and (**D**), and (**C,F**), of the boxed areas in (**B**) and (**E**), respectively. γ and δ, the ventral-most straddler follicles; C1–E1, part of the first arc of vibrissal follicles; I, R, and W are intermediate, red, and white muscle fibers, respectively; ML, fascicles of the *M. maxillolabialis*; NL, fascicles of the *M. nasolabialis*; O, origin of the *M. maxillolabialis*; R, rostral; V, ventral; scale bars = 1 mm in (A), (B), (D), and (E), and 0.1 mm in (C) and (F).

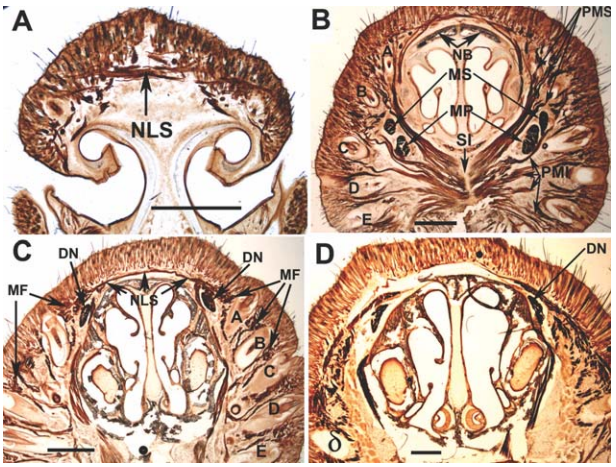

Fig. 3. Coronal slices from the mystacial pad of a 2-week-old Wistar rat. Slices at the level of nasal cartilage (**A**), the 4th vibrissal arc (**B**), the1st vibrissal arc (**C**), and the caudal edge of straddlers (**D**). Slices were stained for CCO activity. **A**–**E**, vibrissa rows; δ, ventral-most straddler; DN, *M. dilator nasi*; MF, transversally sectioned muscle fascicles of the *M. nasolabialis*, and *M. maxillolabialis*; MS and MP, the Partes maxillares superficialis and profunda of the *M. nasolabialis profundus*, respectively; NB, nasal bones; NLS, longitudinally sliced *M. nasolabialis superficialis*; PMI and PMS, Partes mediae inferior and superior, respectively, of the *M. nasolabialis profundus*; SI, *Septum intemusculare*; scale bars = 1 mm.

equivalents (Whitmore, 1999). We used terms that should be relevant to rodent anatomy, such as *rostral, caudal, ventral*, and *dorsal*, instead of *anterior, posterior, inferior*, and *superior*, respectively, which are used in human head anatomy, but that cannot be applied directly to the rodent head structures. In most mammals, muscles of the superficial facial group are striated skeletal muscles innervated by the facial nerve. In the rat, muscles of the mystacial pad constitute only a part of this group. Herein, we shall describe the muscles of the rat mystacial pad, starting from the superficial layers, as illustrated by tissue slices stained for CCO activity.

M. nasolabialis. This muscle originates from the orbital surface of the frontal bone, caudal to the nasofrontal suture, and medial to the medial corner of the eye. It is inserted into the corium of the mystacial pad between the rows of vibrissae. The *M. nasolabialis* appears to be a striated muscle, and its shape is that of a flat divergent muscle. In tangential slices, its fibers fan out rostrally, and just ventrally, to the eye like a broadening sheet (Fig. 2A). It corresponds to the *M. levator labii superioris* and *M. nasolabialis* previously described in mice (Dorfl, 1982) and the golden hamster (Wineski, 1985), respectively. The rostral part of the *M. nasolabialis* turns horizontally. Four of the muscle bundles of the *M. nasolabialis* enter into the mystacial pad between the rows of follicles, one runs dorsal to row A, and another runs ventral to row E. In the mystacial pad, the fibers of this muscle run superficially between the rows of vibrissae in the connective tissue up to the nostril, and their ends are attached to the corium at the rostral border of the mystacial pad. *M. nasolabialis* contained three types of muscle fibers (red, white, and intermediate), that is, could be characterized as a mixed type of muscles (Fig. 2B, C). In coronal slices, transversally-cut bundles of these muscles are seen between the rows of vibrissae just under the corium (Fig. 3C).

M. maxillolabialis. This muscle originates from the maxilla ventral to the infraorbital fissure and caudal to the suture between the premaxilla and maxilla. It is inserted into the mystacial pad. The *M. maxillolabialis* has been described in many rodents (Rinker, 1954) including mice and hamsters, and both Dorfl (1982) and Wineski (1985) refer to it by the same name. The fibers of the *M. maxillolabialis* run divergently in the rostrodorsal direction, and penetrate into the mystacial pad under the fibers of the *M. nasolabialis*. At the caudal edge of the mystacial pad, the fibers of *M. nasolabialis* and *M. maxillolabialis* cross each other (Fig. 2D–F). Within the mystacial pad, the fascicles of the *M. maxillolabialis* turn horizontally in the rostral direction, continue running together with the fascicles of the *M. nasolabialis* between the rows of vibrissal follicles, and contain red, white, and intermediate type of fibers (Fig. 2F). Contraction alone of the *M. maxillolabialis* may pull the caudal part of the mystacial pad in the ventrocaudal direction (provoking a caudal shift of the corium that can be accompanied with a slight rotation of the mystacial pad), whereas its synchronous contraction with the *M. nasolabialis* has a synergistic effect, and

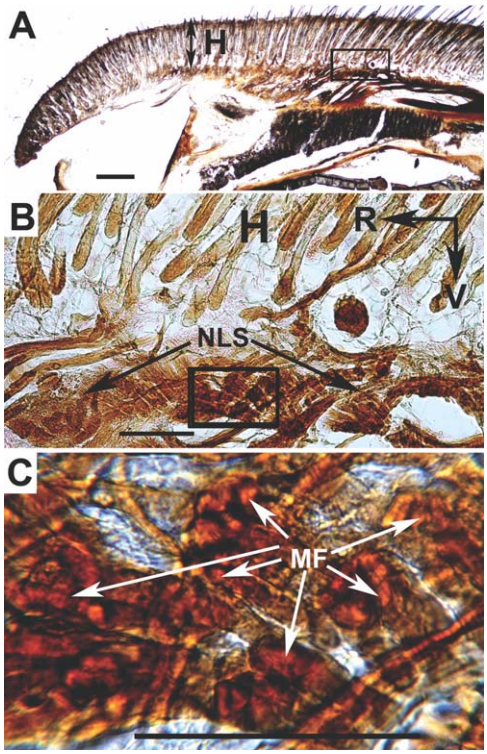

Fig. 4. Parasagittal view of the *M. nasolabialis superficialis* in the mystacial pad of a 3-week-old rat. (**A**) Parasagittal slice of the muzzle stained for CCO activity. (**B**) Enlargement of box in (A). (**C**) Enlargement of box in (B). Muscle fascicles (MF) are cut transversally, and individual muscle fibers are seen (arrows in C). H, the layer of pelagic hairs (derma); NLS, the layer that contains transversally sliced fascicles of the *M. nasolabialis superficialis*; R, rostral; V, ventral. Scale bars = 1, 0.2, and 0.1 mm in panels (A), (B), and (C), respectively.

causes a caudal shift of the corium of the mystacial pad, which results in a retraction of the vibrissae.

M. nasolabialis superficialis. This muscle originates in the fascia along the middorsal line above the nasal bones. It is inserted into the corium of the dorsal part of the mystacial pad within the limits of rows A and B, that is, in the nasal subdivision of the mystacial pad. The fibers of the *M. nasolabialis superficialis* mostly run superficially, and transversally, to the axis of the body, approximately parallel to each other, and can be traced in the dorsal segment of the mystacial pad, including row A (Fig. 3). This muscle corresponds to the *M. transversus nasi* and *M. nasolabialis superficialis* described in mice (Dorfl, 1982) and hamsters (Wineski, 1985), respectively. In parasagittal slices of the rat muzzle, the *M. nasolabialis superficialis* appears as an array of small muscle fascicles running just under the roots of the pelagic hairs that cover the dorsum of the nose (Fig. 4). In the most rostral part of coronal slices, the *M. nasolabialis superficialis* is located above the nasal cartilage (Fig. 3A). In more caudal slices, it runs above the nasal bones, and its fascicles reach the corium at the level of the vibrissa A4 (Fig. 3B). Its fascicles are present in all consecutive coronal slices up to the level of the 1st vibrissal arc (Fig. 3C), but are not seen in coronal slices caudal to the straddlers (Fig. 3D).

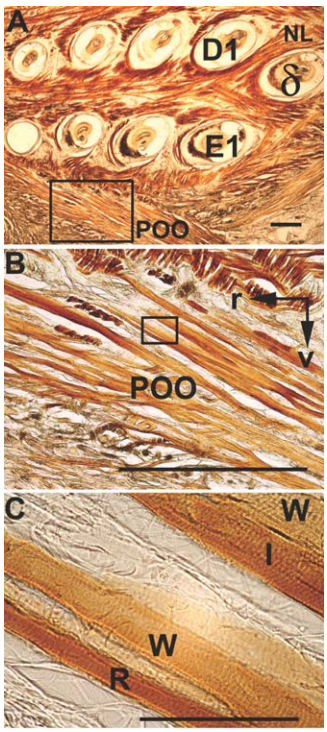

Fig. 5. The Pars orbicularis oris (POO) of the *M. buccinatorius* in a tangential slice (**A**) of an adult Wistar rat mystacial pad stained for CCO activity. (**B**) Enlargement of box in (A). (**C**) Enlargement of box in (B). D1–E1, first follicles of the two ventral vibrissal rows; δ, the ventral-most straddler follicle; I, R, and W are intermediate, red, and white types of muscle fibers; NL, fascicles of the *M. nasolabialis*; r, rostral; v, ventral; scale bar = 1 mm in (A) and (B), and 0.1 mm in (C).

Pars orbicularis oris of the M. buccinatorius. This muscle, which originates from the skin of the lower lip, is inserted into the skin of the upper lip. The *M. buccinatorius* is composed of nine individual muscles (Klingener, 1964; Ryan, 1989), of which the *Pars orbicularis oris* is the only part associated with the mystacial pad. In the golden hamster, the fibers of this muscle are inserted into the mystacial pad, and penetrate between the 2nd and 3rd ventral rows of the vibrissae (Wineski, 1985). In the rat, we observed that the fibers of this muscle, which merged superficially from the lower lip around the angle of the mouth and were inserted into the upper lip, could reach row E of the mystacial pad (Fig. 5A), and in rare cases, also row D. The fascicles of this muscle were composed of loosely-packed muscle fibers, with intervening connective tissue. They contained red, white, and intermediate muscle fibers (Fig. 5B, C).

M. nasolabialis profundus. This muscle is usually described as the one composed of multiple well-differentiated parts, the number of which differed according to the study. For example, only one muscle (*M. nasalis)*, which may be considered as a part of the *M. nasolabialis profundus*, was described in the rostral part of the mouse mystacial pad by Dorfl (1982). Wineski (1985) mentioned five distinct parts (Pars interna, Pars anterior, Pars media superior, Pars media inferior, and Pars maxillaris) in the mystacial pad of the hamster. In other

studies (Rinker 1954; Klingener, 1964; Ryan, 1989), seven parts (Pars interna, Pars media superior, Pars media inferior, Pars anterior, Pars anterior profunda, Pars maxillaris superficialis, and Pars maxillaris profunda) of this muscle were described in mice and other rodents. In the rat mystacial pad, we were able to distinguish seven parts of the *M. nasolabialis profundus*. Five of these parts (Pars media superior, Pars media inferior, Pars maxillaris superficialis, Pars maxillaris profunda, and Pars interna profunda) insert into the mystacial pad, are easily discerned from each other and other muscles, and each part can be considered as a muscle that has a separate well-defined origin and insertion site, and can produce a specific motor effect on the entire mystacial pad or its compartments.

Pars media superior of the M. nasolabialis profundus. This muscle originates from the premaxilla above and between the incisors, dorsal to the origin of the Pars media inferior of the *M. nasolabialis profundus*. The Pars media superior of the *M. nasolabialis profundus* inserts into the corium of the mystacial pad, on both sides of rows A and B. In parasagittal slices, most of the fascicles of this muscle are cut transversally or in an oblique plane, and its fibers run dorsocaudally from the premaxilla at the level of nasal cartilage. In the coronal plane, the muscle fascicles of the Pars media superior divide into three sheets that run divergently, first in the subcapsular zone, then through the plate, and finally, dorsolaterocaudally between the rows of follicles to reach the corium on both sides of follicle rows A and B (Fig. 3B).

Pars media inferior of the M. nasolabialis profundus. This muscle originates from the premaxilla close to the septum intermusculare, at the level of the incisors, and ventral to the origin of the Pars media superior and the Pars maxillaris profunda. The Pars media inferior inserts into the corium of the maxillary subdivision of the mystacial pad. In horizontal plane, muscle fascicles of the Pars media inferior were seen to penetrate the plate, and to run in laterocaudal direction. In tangential slices, its fibers are present in the majority of the slices. The fascicles of the Pars media inferior divide into four sheets that first pass through the subcapsular zone, then through the plate in many places, and continue their way between follicle rows B and C, rows C and D, rows D and E, and finally between row E and the furry buccal pad (Figs. 3B and 6A). In oblique parasagittal slices cut through the plate, four rows of oblique or transversally cut fascicles of the Pars media inferior were observed to penetrate the plate (Fig. 6A). At higher magnification, three types of muscle fibers (red, intermediate, and white) could be seen randomly distributed within each of these muscle fascicles (Figs. 6B–E and 6F–I). In coronal slices, muscle fascicles of the Pars media inferior, as well as of Pars media superior, were seen to enter the corium where they abruptly spread in different directions to form a rosette-shaped final arborization. The rosettes are composed of distal ends of individual muscle cells that fan and finish as thin fibers within a relatively large region of papillary corium. Diverged insertion sites in the corium enlarge the surface of the skin involved in muscle contraction.

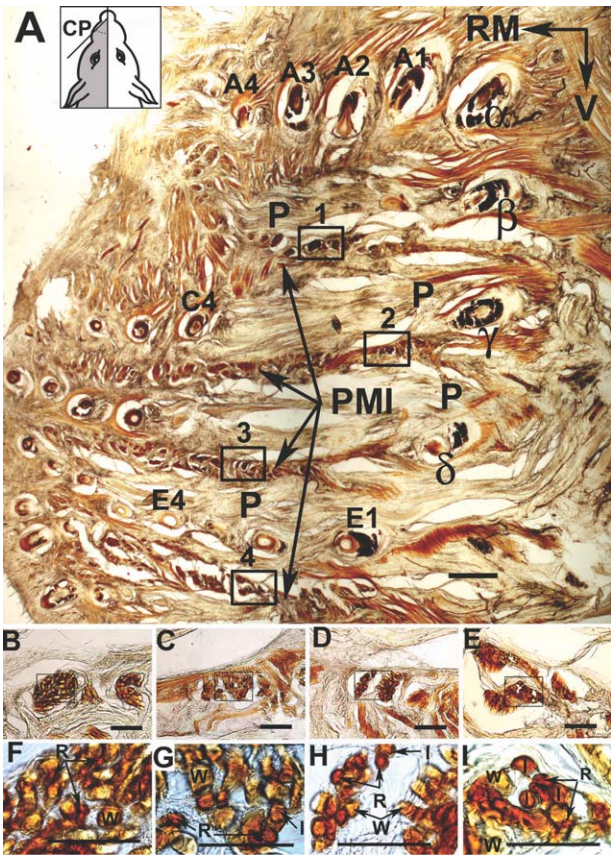

Fig. 6. Pars media inferior (PMI) of the *M. nasolabialis profundus*. (**A**) An oblique parasagittal slice of the mystacial pad of an adult Wistar rat. (**B–E**) Higher magnification of the boxed areas 1–4 in (A), respectively, which represent four sheets of muscle fascicles (arrows in A) of the PMI. (**F–I**) Higher magnification of the boxed areas in (B–E), respectively. α–δ, straddlers; A1–A4, C4, E1, and E4, whisker follicles; I, R, W, intermediate, red, and white muscle fibers, respectively; P, plate; RM, rostromedial; V, ventral; scale bars = 1 mm in (A), 0.2 in (B–E), and 0.1 mm in (F–I). Inset: Schematic drawing of the cutting plane (CP).

A similar configuration of this muscle was described in mice (Dorfl, 1982) as the *M. nasalis*. However, in summarizing papers on rodent musculature (Rinker, 1954; Klingener, 1964; Ryan, 1989), and facial musculature in the golden hamster (Wineski, 1985), this muscle was described as a single sheet composed of muscle fascicles, similar to that of the *M. nasolabialis* and *M. maxillolabialis*. Many papers describing the mystacial pad in rats have utilized Dorfl's proposed image of the mouse *M. nasalis* (see Fig. 1 in Dorfl, 1982). However, in rats, there are only four sheets in the Pars media inferior, which are clearly seen in coronal slices on both sides of the rows C–E of the rat mystacial pad (Figs. 3B and 6A), not five as shown in mice by Dorfl (1982). Contraction of the Pars media inferior should provide a rostral shift of the corium of the maxillary part of the mystacial pad, which would cause whisker protraction. Simultaneously, its contraction should also diminish, according to the direction of the muscle fibers, the angle between the whiskers of rows C, D, and E, which would result in a more converged whisker position in the protracted whisker array.

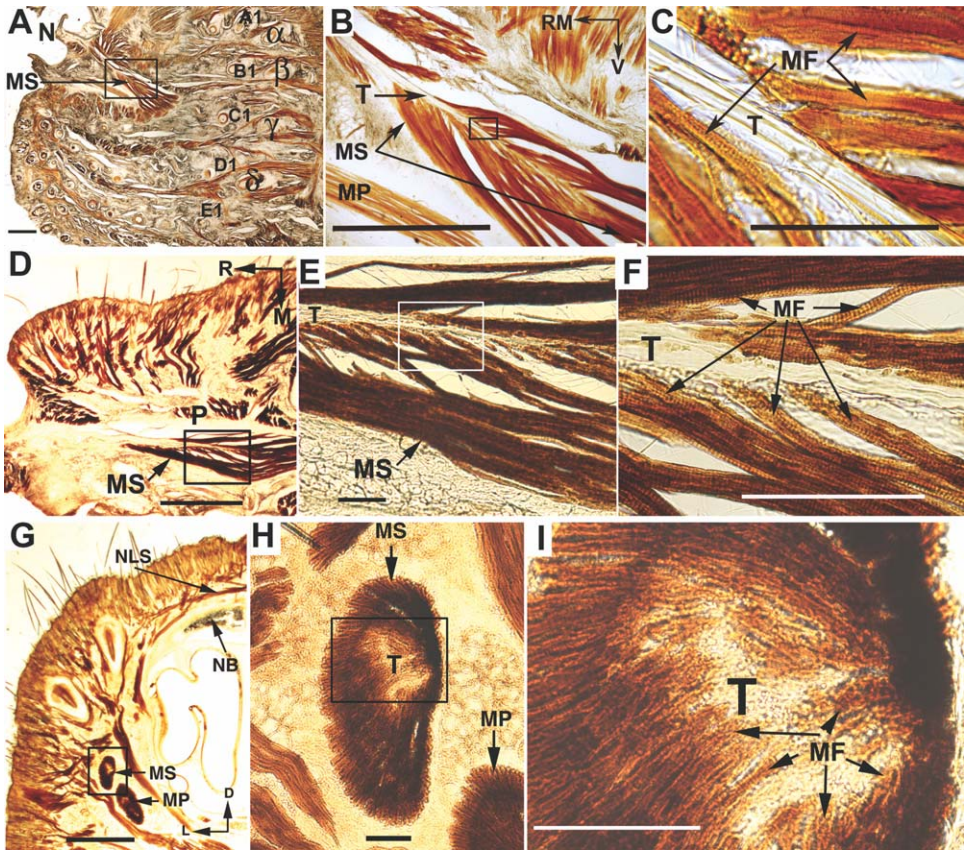

Fig. 7. Depiction of the Pars maxillaris superficialis (MS) of the *M. nasolabialis profundus* in different cutting planes. An oblique parasagittal slice (**A–C**), a horizontal slice (**D–F**), and a coronal slice (**G–I**) of the mystacial pad of an adult rat. (B,E,H) Higher magnification of the boxes in (A,D,G), and (C,F,I), of the boxes in (B,E,H), respectively. α–δ, straddlers; A1–E1, the first arc of the five rows of vibrissal follicles; D, dorsal; L, lateral; M, medial; MF, muscle fibers; MP, Partes maxillares profunda; MS, Partes maxillares profunda superficialis; P, plate; R, rostral; RM, rostromedial; T, tendon; and V, ventral. Scale bars = 1 mm in (A), (B), (D), and (G), and 0.1 mm in (C), (E), (F), (H), and (I).

Pars maxillaris superficialis of the M. nasolabialis profundus. This muscle derives from a tendon that originates from the dorsolateral part of the nasal cartilage and the premaxilla caudal to the nasal passage. The placement and characteristics of this muscle differ in various rodents. In hamsters, this muscle was described as the one running in the subcapsular zone (Wineski, 1985). In rats, in lateral-to-medially cut consecutive oblique slices, the Pars maxillaris superficialis appeared after a few slices that contained the plate, and had an apparently bipennate structure (Fig. 7A–C). In horizontally cut slices, Pars maxillaries superficialis had a similar appearance: centrally positioned branching tendon and bilaterally attached muscle fibers (Fig. 7D–F). In coronal plane, it appeared as an oval structure with several central tendons, and radially directed muscle fibers (Fig. 7G–I). So, this rat muscle has a multipennate structure, and starts off rostrally as a smooth tendon to which muscle fibers attach circumferentially at an acute angle, as revealed in oblique tangential and horizontal slices. At the level of the third and forth vibrissal arcs, the tendon disappears, and muscle fibers spread mostly in dorsoventral direction. These muscle fibers are organized into large, tightly-packed fascicles, with little intervening connective tissue. In rats, the Pars maxillaris superficialis runs caudally within the subcapsular zone up to the first vibrissal arc, and is inserted into the inner surface of the plate.

Pars maxillaris profunda of the M. nasolabialis profundus. This muscle originates as a short tendon on the lateral side of the nasal cartilage, ventral to the nostril and to the origin of the Pars maxillaris superficialis. The Pars maxillaris profunda inserts into the caudal part of the plate. It runs deeper than the Pars maxillaris superficialis (Figs. 3B and 8A, B). Like the Pars maxillaris superficialis, the Pars maxillaris profunda is represented by a multipennate muscle, and appears in oblique tangential slices together with (in a few consecutive slices), or immediately after, the Pars maxillaris superficialis (Fig. 8A). Each of the maxillary parts contained a tendon that was centrally oriented, with circumferential attachment of muscle fibers (Fig. 7A–I). In deeper oblique tangential slices, both maxillary parts can be seen superimposed on each other (Fig. 8B). The majority of the fibers of both maxillary parts are seen under the plate, with tightly-packed fascicles, and their most caudal ends appear to fuse with the plate at the level of the first vibrissal arc and straddlers.

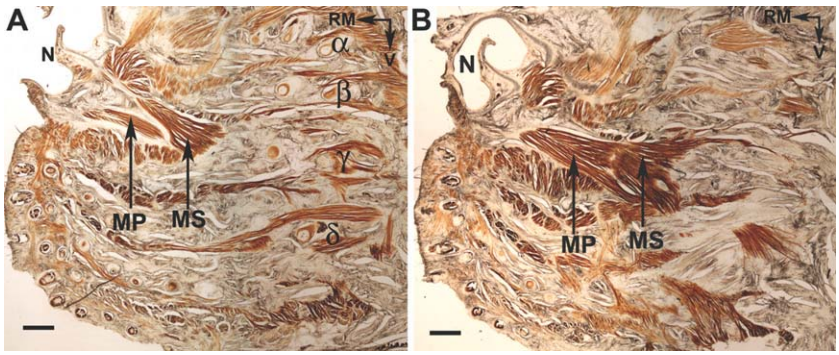

Fig. 8. Oblique parasagittal slices (120 μm apart) of the adult Wistar rat mystacial pad in which the Partes maxillares superficialis and profunda (MS and MP, respectively) of the *M. nasolabialis profundus* are evident. Slices were stained for CO activity. Panel (**A**) is more superficial than the panel (**B**). α–δ, straddlers; N, nostril; RM, rostromedial; V, ventral; scale bars = 1 mm.

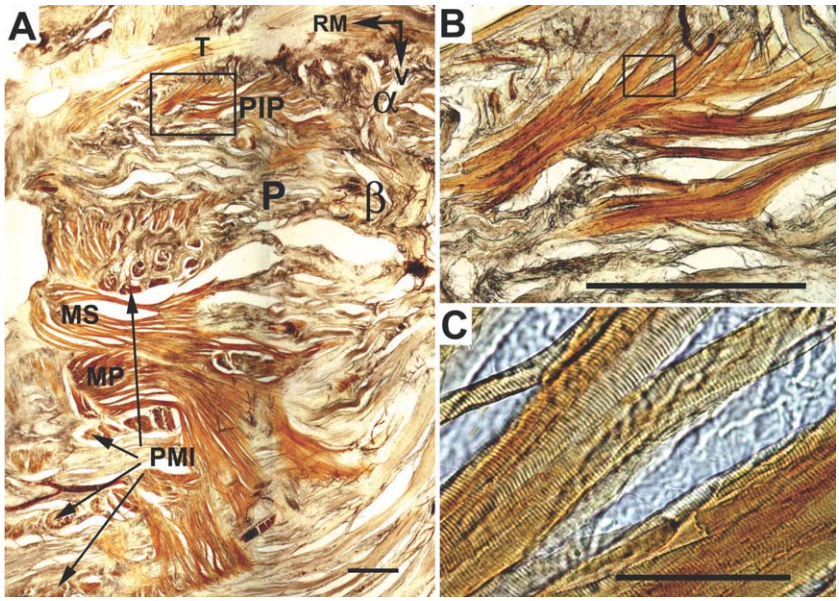

Fig. 9. Pars interna profunda of the *M. nasolabialis profundus*. (**A**) An oblique parasagittal slice of an adult Wistar rat. (**B**) Enlargement of the boxed area in (A). (**C**) Enlargement of the boxed area in (B). α and β, straddlers; MP and MS, Partes maxillares profunda and superficialis, respectively, of the *M. nasolabialis profundus*; P, plate; PIP, Pars interna profunda of the *M. nasolabialis profundus*; PMI, Pars media inferior of the *M. nasolabialis profundus*, represented by four sheets (arrows) of transversally cut muscle bundles; RM, rostromedial; T, tendon of the *M. dilator nasi*; V, ventral; scale bars = 1 mm in (A) and (B), and 0.1 mm in (C).

Pars interna profunda of the M. nasolabialis profundus. This muscle is the deepest of the three known parts of the Pars interna of the *M. nasolabialis profundus* (Rinker, 1954). It originates as a short flat tendon from the dorsolateral part of the nasal cartilage, and inserts into the plate of the nasal subdivision of the mystacial pad. This muscle has a triangular shape, runs in caudal direction within subcapsular zone up to the first vibrissal arc, and is composed of mostly white and intermediate muscle fibers (Fig. 9C). We are unaware of any published descriptions of the Pars interna profunda in Wistar rats, so we have named this muscle according to its topographic position. Contraction of the Pars interna profunda pools the dorsal part of the plate rostral and causes retraction of the whiskers of rows A and B.

Intrinsic Muscles

In the rat, the four superficial extrinsic muscles and the five parts of the *M. nasolabialis profundus* described above were all inserted into the plate or into the corium of the mystacial pad between the rows of follicles. In contrast, the intrinsic muscles were associated with vibrissa follicles and were only partially inserted into the corium. The majority of the intrinsic muscles of the rat mystacial pad were connected to each of two adjacent follicles of the same row. These muscles resembled slings that embraced the lower half of the rostral follicle of every follicle pair, similarly to the descriptions of intrinsic muscles in mice (Dorfl, 1982) and hamsters (Wineski, 1985). In tangential slices, only part of each intrinsic muscle could be visualized (Fig. 10A). Entire intrinsic

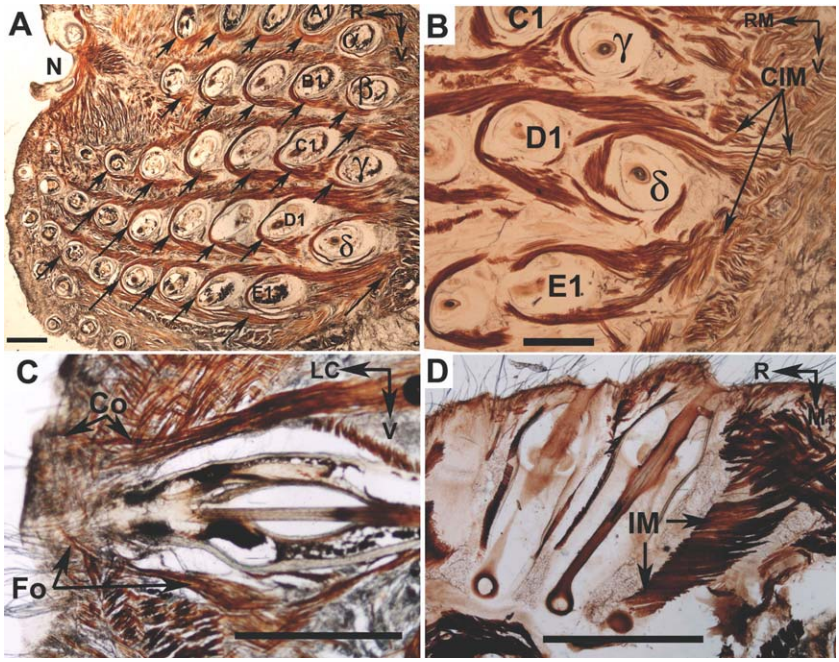

Fig. 10. Intrinsic muscles of the adult Wistar rat mystacial pad. (**A**) A tangential slice containing a whole set of intrinsic muscles, each of which is indicated by an arrow. Most of the muscle slings are only partially represented in this plane. (**B**) An oblique slice with the most caudal extremities of intrinsic muscles (CIM). C1–E1 are the most caudal vibrissae of rows C–E. (**C**) Distal end of a follicle cut in the oblique plane. The extremities of an intrinsic muscle are attached to the follicle (Fo), and partially to the corium (Co). In a horizontal slice (**D**), two complete adjacent follicles are clearly seen. Part of an intrinsic muscle (IM) covers about half of the follicle. Slices were stained for CO activity. α, β, γ, δ, straddlers; A1–E1, the first arc of the five vibrissal rows; LC, laterocaudal; M, medial; N, nostril; R, rostral; RM, rostromedial; V, ventral; scale bars = 1 mm.

muscles could only be seen in oblique slices, where the cutting plane was parallel to the direction of the muscle extremities. For most caudal follicles (α, β, γ, δ, A1, B1, C1, D1, and E1), the extremities of the intrinsic muscles merged with the fibers of the *M. nasolabialis* and *M. maxillolabialis*, and were partially inserted into the corium (Fig. 10B). The extremities of each sling-shaped intrinsic muscle were attached mainly to the lateral faces of the distal part of the caudal member of each follicle pair. A small portion of the extremity of each intrinsic muscle was inserted into the corium close to the upper part of the caudal follicle (Fig. 10C). The size of the intrinsic muscles correlated with the size of their associated follicle. Intrinsic muscles were observed around all the follicles of the straddlers, row A, and row B, and around the first six or seven follicles of rows C, D, and E. In horizontal slices that were cut parallel to the long axis of the follicles (clearest for rows D and E), intrinsic muscles appeared as thin layers of muscle fibers between two neighboring follicles in a row (Fig. 10D). Intrinsic muscles expressed low levels of CCO activity, and contained mainly white fibers, with a few red and intermediate fibers observable along muscle extremities (Fig. 11A–C). Our findings with regard to fiber types in extrinsic and intrinsic mystacial muscles and to amounts of CCO activity in muscle fibers are in agreement with those of other groups (Gauthier, 1969; Padykula and Gautier, 1970; Gautier and Dunn, 1973; Niederle and Mayr, 1978; White and Vaughan, 1991; Jin et al., 2004).

Compartmentalization of Muscle Distribution Within the Rat Mystacial Pad

As a functional sensor and effector module, the rat mystacial pad is anatomically represented by five vibrissal rows that are apparently similar with regard to their morphology. However, of the four extrinsic mystacial pad muscles and of five parts of the *M. nasolabialis profundus* described above, only two (the *M. nasolabialis* and *M. maxillolabialis*) appear to be evenly inserted into the whole mystacial pad. Another three extrinsic muscles (the *M. nasolabialis superficialis*, the Pars media superior and Pars interna profunda of the *M. nasolabialis profundus*) are inserted only into the dorsal part of the mystacial pad that involves rows A and B (the nasal subdivision of the mystacial pad). The other four extrinsic muscles (the Pars orbicularis oris of the *M. buccinatorius*; the Pars media inferior, Pars maxillaris superficialis, and Pars maxillaris profunda of the *M. nasolabialis profundus*) appear to be inserted only into the ventral part of the mystacial pad that involves rows C, D, and E (the maxillary subdivision of the mystacial pad). In both 2-week-old and adult rats, the rostral part of vibrissal row B was separated from row C by a much wider space than between the other rows (see Figs. 1, 2D, 3B, and 10A). Tangential and coronal cutting of the mystacial pad revealed that the fibers of the three sheets of the Pars media superior of the *M. nasolabialis profundus* are attached to the corium on both sides of the dorsal-most vibrissae, that is, the vibrissae of rows A and B. Another muscle, the Pars

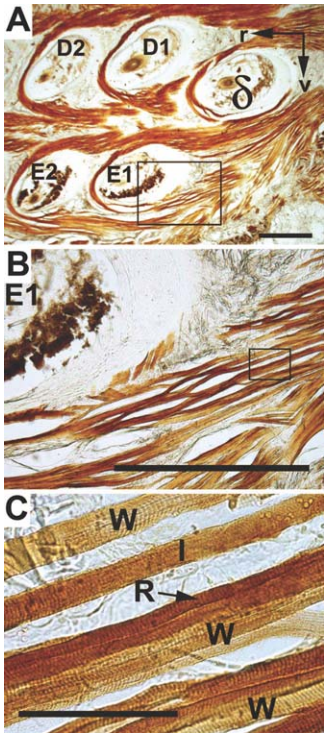

Fig. 11. Muscle fiber types in intrinsic muscles of the rat mystacial pad. (**A**) A parasagittal slice representing intrinsic muscles of the ventrocaudal part of the mystacial pad. (**B**) Enlargement of box in (A). (**C**) Enlargement of box in (B). D1, D2, E1, and E2, vibrissal follicles; δ, follicle of the most ventral straddler; I, R, and W are intermediate, red, and white muscle fibers, respectively; r, rostral; v, ventral; scale bars = 1 mm in (A) and (B), and 0.1 mm in (C).

media inferior of the *M. nasolabialis profundus*, which is an analog of the nasal muscle described in mice (Dorfl, 1982), is attached to the corium on both sides of rows C, D, and E. So, in the rostral part of the space between rows B and C, two sheets of muscles (one from the Pars media superior and the other from the Pars media inferior of the *M. nasolabialis profundus*) pass through and eventually reach the corium through this space in the caudolateral direction. We conjecture that the architecture of mystacial pad muscles in adult rats reflects stages of the embryonic development of the mystacial pad. For example, in 14-day-old Wistar rat embryos (Fig. 12), only the maxillary subdivision (the ridges of rudimental rows C–E, and the rudiments of the straddlers γ and δ) of the mystacial pad is clearly differentiated, and the nasal subdivision develops later.

DISCUSSION

Methodological Considerations

Most of our knowledge about muscle architecture in general, and about facial musculature in rodents in particular, was obtained using dissection as the principal traditional methodological approach (Huber, 1930a,b; Rinker, 1954; Klingener, 1964; Ryan, 1989). The main advantage of this method is being able to observe the whole length of individual muscles, from their origin (the site of attachment to bone or cartilage) to the site of their insertion, or vice versa, during dissection. Dissection yields precise and

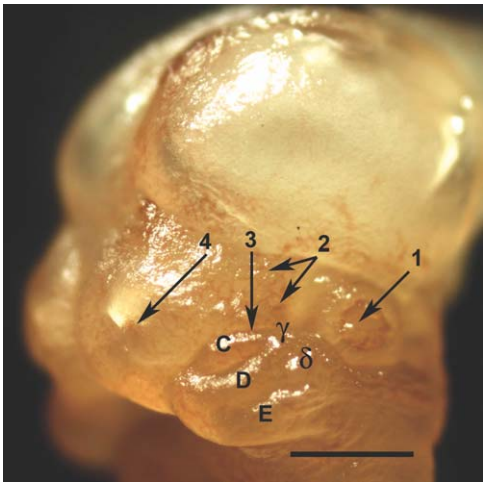

Fig. 12. Maxillary subdivision of the mystacial pad in a 14-day-old Wistar rat embryo. C–E, rudiments of vibrissal rows in the maxillary prominence; γ and δ, the rudiments of the two ventral-most straddlers; 1, eye; 2, relatively flat surface of the lateral nasal prominence; 3, nasolacrimal groove; 4, nostril; scale bar = 1 mm.

reliable information for skeletal muscles and for most large facial muscles. However, this method often encounters difficulties when studying intrinsic and extrinsic mystacial muscles, as well as small skeletal muscles, because of the physical properties of these tissues, and of variable spatial relationships between different tissue components, even when dissecting microscopes are utilized.

For the purposes of this study, slicing of frozen facial tissues *in situ*, followed by staining of consecutive slices for CCO activity, was chosen because of having a few obvious advantages: (a) preservation of the natural spatial relationships between the tissue components; (b) visualization of individual muscle fibers which enables detection of the smallest muscles and individual muscle cells (fibers); (c) obtaining of a qualitative information about the type of muscle fibers and about their quantitative relationship within each individual muscle fascicle; (d) facilitated identification of the sites of origin and insertion for small muscles.

Muscle Arrangement within the Rodent Mystacial Pad

Previously, we observed that the patterns of vibrissa arrangement in rodents, such as mice, rats, golden hamsters, and guinea pigs, are similar (Haidarliu and Ahissar, 1997). This similarity, which has led to the same principles of classification and nomenclature being used with regard to vibrissa in these species of rodents, was further reflected in our current proposal on muscle architecture of the rat mystacial pad. In fact, similarities in the facial muscle architecture of various mammals were described as early as 1930 (Huber, 1930a,b). So far, a detailed description of the musculature of the mystacial pad has only been provided for the mouse (Dorfl, 1982) and golden hamster (Wineski, 1985). For these two species of rodents, the arrangement of the mystacial muscles, and their nomenclature, are not identical. Of all the extrinsic muscles, only one (*M. maxillolabialis)* had the same name. The other two extrinsic muscles

that are anatomically the same, had different names: *M. levator labii superioris* and *M. transversus nasi* in mice, which correspond to *M. nasolabialis and M. nasolabialis superficialis* in the golden hamster. The *M. nasalis* described in mice (Dorfl, 1982) has no analog in descriptions of hamster musculature (Wineski, 1985) or of rodent myology (see fundamental papers by Huber, 1930a,b; Rinker, 1954; Klingener, 1964; Ryan,1989).

The most contradictory data concern descriptions of parts of the *M. nasolabialis profundus*, of which a few are inserted into the mystacial pad. Originally, three parts of the *M. nasolabialis profundus* (the Pars media superior, Pars media inferior, and Pars anterior profunda) were described as being inserted into the mystacial pad of rodents (Rinker, 1954). Later, only two parts of the *M. nasolabialis profundus* were shown to be related to the mystacial pad (the Pars media inferior and Pars maxillaris profunda) (Klingener, 1964). One study on musclature of the mouse mystacial pad (Dorfl, 1982) did not mention the *M. nasolabialis profundus* at all. Muscle fibers were observed entering the murine mystacial pad from only one part of *M. nasolabialis profundus*, the Pars media superior (Ryan, 1989). In hamsters, three parts (the Pars media superior, Pars media inferior, and Pars maxillaris) of the *M. nasolabialis profundus* are inserted into connective tissue of the mystacial pad (Wineski, 1985). In the rat, we found that five parts of the *M. nasolabialis profundus* (the Partes mediae superior and inferior, the Partes maxillares superficialis and profunda, and the Pars interna profunda) are inserted into the mystacial pad.

In rodents, observed differences in the roles in whisker movement of different parts of the *M. nasolabialis profundus* could be due to interspecies variability. Therefore, we tried to clarify how our findings correspond to the observations of other groups with regard to the other extrinsic muscles of the rat mystacial pad. Dorfl's diagram of the mouse *M. nasalis* (Dorfl, 1982) was used in many papers to show how it participates in whisking in rats (Guntinas-Lichius et al., 2005; Angelov et al., 2007; Hill et al., 2008). In the rat, muscle activity from intrinsic or extrinsic muscles was recorded, and these muscles were stimulated (Berg and Kleinfeld, 2003; Hill et al., 2008). From these studies, it is now evident that in the rostral part of the mystacial pad, the effect of electrode stimulation depends on the localization of the inserted electrode and on the size of the exposed electrode tip. If the electrode tip is localized in the Pars media inferior, then the stimulation causes whisker protraction. However, if the electrode tip is in the Pars maxillaris superficialis or profunda, which are close to each other, then the opposite occurs, that is, retraction. Thus, when recording from the mystacial pads of rodents, the exact position of the electrode tip used for recording should be verified by stimulation (see Carvell et al., 1991; Berg and Kleinfeld, 2003; Shaw and Liao, 2005). However, this is impossible in the rostral part of the mystacial pad if the electrode tip exceeds a few tens of microns, because muscles with opposite stimulation effects are located very close to each other.

Anatomical, Developmental, and Functional Data that Support Compartmentalization of the Mystacial Pad

Division of the rat mystacial pad into two compartments has been proposed based on differences in the distribution of muscles within the ventral and dorsal portions of the rat mystacial pad, as well as, on a larger space separating the muscles between rows B and C of vibrissae. This subdivision is supported by the following. During embryonic development of mice, muscles associated with rows A and B of vibrissae develop from the lateral nasal prominence, while rows C, D, and E originate from the maxillary prominence, as observed in 12-day-old embryos (Yamakado and Yohro, 1979; Van Exan and Hardy, 1980). Similarly, in rat embryos, vibrissal ridges become visible on the 13th day of development, and vibrissal rows are detected on the snout by the 14th day, becoming distinct on the 15th day (Erzurumlu and Jhaveri, 1992). However, mystacial pad compartmentalization was not dealt with in that study. Indirect evidence of differences in the development of the two mystacial pad subdivisions is that in day 15 rat embryos, the fascicles of axons from the maxillary nerve fan out mainly toward rows C, D, and E of vibrissae (see Erzurumlu and Killackey, 1983). In mice, formation of vibrissal ridges and follicle rudiments was observed first in the maxillary prominence (Wrenn and Wessells, 1984), which is supported by our finding that in 14-day-old Wistar rat embryos, vibrissal ridges are only detected in the maxillary compartment (Fig. 12).

We propose that the anatomical differences between nasal and maxillary subdivisions of the rat mystacial pad, revealed in the present study, are the basis of functional differences. In our study of vibrissal kinematics in 3D, we described horizontal and vertical translation of the whisker base, as well as an unknown torsional rotation of the whisker shaft, in the nasal and maxillary regions of the mystacial pad, such that rows A and E counter rotate (Knutsen et al., 2008). When an object touches the upper whiskers of a rat, that is, the whiskers of the rows A or B, it is reasonable to assume that further search or foveal whisking is performed mainly with these whiskers. This should be possible because the muscle fibers of the Pars media superior and Pars interna profunda of the *M. nasolabialis profundus* reach the corium and the plate, respectively, that surround only rows A and B, and the *M. nasolabialis superficialis* is also inserted into the corium of the nasal vibrissal compartment. If an object touches the vibrissae of rows C–E, these vibrissae can also be moved in different planes by muscles that reach only this region (the Pars media inferior, the Partes maxillares superficialis and profunda of the *M. nasolabialis profundus*, and the Pars orbicularis oris of the *M. buccinatorius*). Involvement in whisker movement of muscles other than intrinsic ones is supported by the independence, with regard to the direction of their movements, of some individual whiskers within the array (Sachdev et al., 2002).

Effects of Muscle Architecture on Vibrissa Dynamics

The rat vibrissal system is excellently adapted to detect objects in the vicinity of the head, and to determine their structure. The motor plant of the mystacial pad is equipped with vibrissae, vibrissal follicles, muscles, and elastic elements of connective tissue. Physical properties of the tissues of the mystacial pad permit quick whisker movements with large amplitudes, with the muscles of the pad being among the quickest

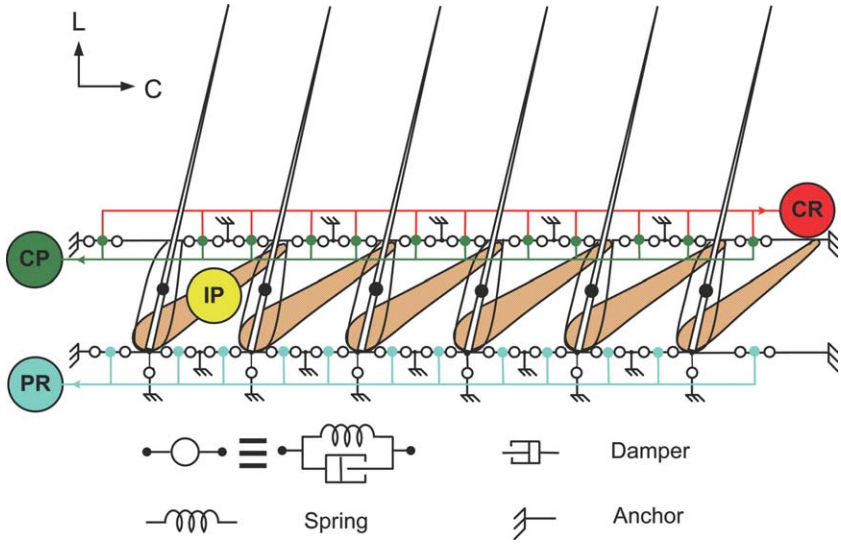

Fig. 13. Schematic drawing of a biomechanical model representing one vibrissal row in the maxillary compartment of the rat mystacial pad in resting position. Intrinsic whisker protractors (IP) represent intrinsic muscles. The corium whisker protractor (CP) represents the Pars media inferior of an extrinsic muscle *(M. nasolabialis profundus)*. The corium whisker retractor (CR) represents two extrinsic muscles (the *M. maxillolabialis* and *M. nasolabialis*). The plate whisker retractor (PR) represents the Partes maxillares superficialis and profunda of the *M. nasilabialis profundus*. Green dots in the upper (corium), and blue dots in the bottom (plate) rows represent attachment sites of the extrinsic muscles. Large black dots represent the vibrissal centers of mass. Empty circles represent springs coupled with dampers which symbolize the elasticity of the tissue. Anchors represent non elastic sites in the mystacial pad. C, caudal; L, lateral.

muscles observed so far (Jin et al., 2004). This quick motor activity of vibrissal muscles is possible due to the large supply of ATP available to these muscles under both aerobic and anaerobic conditions.

Based on the origin and insertion sites of mystacial pad muscles, as well as their functional relationships described in the current study, we propose a reduced, 2D biomechanical model of a vibrissal row in the rat mystacial pad motor plant (Fig. 13). This model demonstrates the mechanics of interactions within a row of vibrissal follicles in the maxillary compartment (rows C–E) of the rat mystacial pad. Based on our current anatomical work, and a previous modeling study (Hill et al., 2008), we suggest that during regular exploratory whisking, whisker protraction is mainly due to contraction of intrinsic muscles (intrinsic whisker protractor) that are wrapped around the lower part of the rostral follicle, and extend their extremities to the upper part of the neighboring caudal follicle, as well as to the corium in the whisker vicinity. Thus, each whisker is protracted by two intrinsic muscles.

Extrinsic muscles that protract vibrissae (corium whisker protractor) are represented by the bundles of the Partes mediae superior and inferior of the *M. nasolabialis profundus*, which fan out radially from their rostrally-located origins. Contraction of these muscles provides a rostral pulling of the corium, and may cause whiskers to converge when they reach their rostral-most position during protraction. Such whisker dynamics can increase resolution of object scanning, and is reminiscent of the whisker behavior described by Berg and Kleinfeld (2003), which consists of two general modes of whisking (exploratory and foveal). Exploratory whisking consists of whisking bouts of rostrocaudal sweeps with large amplitudes. In contrast, during foveal whisking, which occurs while searching for food, the vibrissae mainly thrust forward to form a dense pattern, and the whisking bouts are of lower amplitude and higher frequency. Rats can also increase the number of surface contacts with an unexpected object by reducing whisker spread (Grant et al., 2009). We suggest that during regular whisking in the air, or during exploratory whisking characterized by large rhythmic repetitive rostrocaudal sweeps, intrinsic muscles play a dominant role. According to this paradigm, after the first unexpected whisker contact or during active search for food, median parts of deep nasolabial muscles are involved, which leads to reduction of whisker spread or maintains foveal whisking.

Whisker dynamics strongly depends on the combination of muscles involved in each movement. For example, whisker retraction can be caused by two groups of muscles, the corium whisker retractor muscles (*M. nasolabialis* and *M. maxillolabialis*), and the plate whisker retractor muscles (Partes maxillares superficialis and profunda, and Pars interna profunda of the *M. nasolabialis profundus*), as well as by elastic elements of the mystacial pad both in the corium and in the plate. We suppose that the trajectory and temporal characteristics of such a retraction is determined by a combination of these synergistic muscles and by the degree of their activation. However, if the muscle combination involves antagonistic muscles, the effect of their contraction may be qualitatively different. For example, simultaneous contraction of the Pars media inferior (corium whisker protractor) with the Pars maxillaris superficialis and/or Pars maxillaris profunda of the *M. nasolabialis profundus* (plate whisker retractor) can provide a translational effect in the rostral direction, with or without changes in the whisker angle, which depends on the degree of contraction of these muscles.

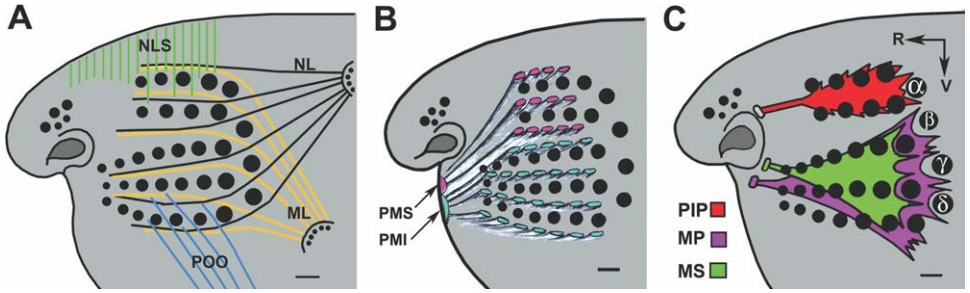

Fig. 14. Schematic representation of muscles inserted into the rat mystacial pad. Superficial muscles (**A**): *M. maxillolabialis* (ML), *M. nasolabialis* (NL), *M. nasolabialis superficialis* (NLS), and Pars orbicularis oris of the *M. buccinatorius* (POO). Deep protracting and "focusing" vibrissae muscles (**B**): Pars media inferior (PMI) and Pars media superior (PMS) of the *M. nasolabialis profundus*. Deep retracting vibrissal muscles (**C**): Pars interna profunda (PIP), Pars maxillaris profunda (MP) and Pars maxillaris superficialis (MS) of the *M. nasolabialis profundus*. α–δ, straddlers; R, rostral; V, ventral; scale bars = 1 mm.

TABLE 1. Expected effects of the contraction of individual muscles of the rat mystacial pad

Muscle	Level	Expected effect of muscle contraction	Whisker operator
Nasolabialis	Superficial	Pulling the corium of the mystacial pad dorsocaudal. Vibrissa retraction.	CR
Maxillolabialis	Superficial	Pulling the corium of the mystacial pad ventrocaudal. Vibrissa retraction.	CR
Nasolabialis superficialis	Superficial	Dorsal pulling of the corium. Elevation of the vibrissal rows A and B.	CE
Buccinatorius Pars orbicularis oris	Superficial	Pulling maxillary subdivision of the mystacial pad downward. Ventrocaudal deflection of vibrissal rows C–E.	VD
Nasolabialis profundus			
Pars media superior	Radial	Rostral pulling of the corium of the nasal subdivision of the mystacial pad. Protraction and convergence of vibrissal rows A and B.	CP
Pars media inferior	Radial	Rostral pulling of the corium of the maxillary subdivision of the mystacial pad. Protraction and convergence of vibrissal rows C – E.	CP
Pars interna profunda	Deep	Rostral pulling of the plate. Retraction of vibrissal rows A and B	PR
Pars maxillaris superficialis	Deep	Pulling the plate rostral. Retraction of vibrissal rows C–E.	PR
Pars maxillaris profunda	Deep	Pulling the plate rostral. Retraction of vibrissal rows C–E.	PR
Intrinsic muscles	Radial	Rostral pulling of the distal follicular ends and the corium, and caudal pulling of the proximal follicular ends and the plate. Follicle rotation around dorsoventral axis and whisker protraction.	CP + PP

Whisker operators: CE, corium whisker elevator; CP, corium whisker protractor; CR, corium whisker retractor; PP, plate whisker protractor; PR, plate whisker retractor; VD, ventrocaudal whisker deflector.

All muscles of the rat mystacial pad can be classified into either superficial or deep, as schematically depicted in Fig. 14. The rat mystacial pad is equipped with two superficial muscles (the *M. nasolabialis superficialis* and the Pars orbicularis oris of the *M. buccinatorius)* that can cause deviation, via muscle contraction, from the main rostrocaudal whisking trajectory. During whisking, changes in the plane of whisker trajectories during rostrocaudal movement are probably the result of the *M. nasolabialis superficialis* pulling rows A and B in the dorsal direction, while the Pars orbicularis oris deflects the whiskers of the rows C–E ventrally. Thus, trajectories generated by single whiskers can be described as occupying an expanded two-dimensional space. In fact, upon two-dimensional monitoring of whisker movements, whisking trajectories were shown to possess a dominating rostrocaudal component and a less pronounced dorsoventral component (Bermejo et al., 2002). A significant increase in the efficiency of whisking behavior is the result of 2D mystacial pad translation movements (Bermejo et al., 2005).

Our results suggest that the muscular architecture and dynamics in the rodent mystacial pad should be analyzed in three dimensions of space. According to which, the effect of a muscle contraction should be determined not only by the sites of its origin and insertion, but also by the geometry and essential properties of the muscles. For example, contraction of the Partes maxillares superficialis and profunda of the *M. nasolabialis profundus* pulls the plate of the mystacial pad in the rostral direction. As a result, the plate pulls, also rostrally, the proximal ends of the vibrissa follicles, while the whiskers are

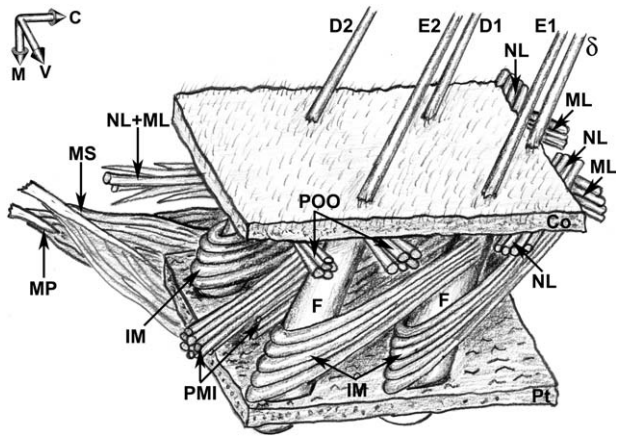

Fig. 15. Schematic drawing of part of the ventrocaudal compartment of the rat mystacial pad. C, caudal; Co, corium; δ, the ventralmost straddler; D1, D2, E1, E2, vibrissae; F, follicles; IM, intrinsic muscles; M, medial; ML, *M. maxillolabialis*; MP and MS, Partes maxillares profunda and superficialis, respectively, of the *M. nasolabialis profundus*; NL, *M. nasolabialis*; PMI, Pars media inferior of *the M. nasolabialis profundus*; POO, Pars orbicularis oris of the *M. buccinatorius*; Pt, plate; V, ventral.

being retracted, that is, are deflected in the opposite, caudal direction. The expected effects of contraction of individual muscles on the dynamics of the mystacial pad, its structural elements, and vibrissal behavior are listed according to the anatomical position of the muscles within the mystacial pad, as well as their sites of origin and insertion (Table 1). Individual deep extrinsic muscles can cause both protraction and retraction of the vibrissae, as well as rotation of the mystacial pad or its parts. Simultaneous contraction of the muscles that are inserted into the corium and into the plate provides a translational effect or produce a functional displacement of the muscle insertion sites. Anatomical relationships of the mystacial pad muscles described in this study are depicted in a 3D schematic drawing (Fig. 15). Viewing the rat mystacial pad musculature as a 3D entity should facilitate understanding phenomena such as divergent movement of adjacent whiskers (Sachdev et al., 2002), foveal whisking (Berg and Kleinfeld, 2003), torsional rotation of whiskers (Knutsen et al., 2008), and changes in whisker spread (Grant et al., 2009).

CONCLUSIONS

Understanding of active tactile sensing requires detailed information about the motor plant(s) involved. Here, we describe in detail, for the first time, the muscles of the rat mystacial pad controlling whisker movement. The principles of muscle architecture relevant to large and synchronous rostrocaudal whisker sweeps (whisking) in rat are similar to those previously described for the mouse and hamster, except for one rostral muscular system that induces whisker retraction (the Pars interna profunda and two maxillary parts of the *M. nasolabialis profundus* that pull the plate of the rat mystacial pad). The ability, that we show here, of the other two deep extrinsic muscles (P. media superior and Pars media inferior of the *M. nasolabialis profundus*) to control the spread of the whisker array is most likely used by the rat to modulate the spatial sampling resolution according to the needs. This function might prove efficient, as the thin whiskers sample only a tiny portion of the space around the rat snout. Likely, bio-mimetic models of whiskered robots might find such dynamic focusing function an efficient solution for addressing various volumes and objects with various sizes and granularities, using the same number of whiskers. Our anatomical and developmental analyses indicate a row-wise submodularity of the musculature of vibrissal rows A–B and rows C–E, which suggest separate, though coordinated, control systems for the muscles within each pad; such decoupling might also prove beneficial for robotics when trying to sense the floor and the ceiling of a cavity simultaneously.

ACKNOWLEDGMENTS

Ehud Ahissar holds the Helen Diller Family Professorial Chair of Neurobiology. The authors thank Dr. Barbara Schick for reviewing the manuscript.

LITERATURE CITED

Angelov DN, Ceynowa M, Guntinas-Lichius O, Streppel M, Grosheva M, Kiryakova SI, Skouras E, Maegele M, Irintchev A, Neiss WF, Sinis N, Alvanou A, Dunlop SA. 2007. Mechanical stimulation of paralyzed vibrissal muscles following facial nerve injury in adult rat promotes full recovery of whisking. Neurobiol Dis 26:229–242.

Berg RW, Kleinfeld D. 2003. Rhythmic whisking by rat: retraction as well as protraction of the vibrissae is under active muscular control. J Neurophysiol 89:104–117.

Bermejo R, Friedman W, Zeigler HP. 2005. Topography of whisking. II: Interaction of whisker and pad. Somatosens Mot Res 22:213–220.

Bermejo R, Vyas A, Zeigler HP. 2002. Topography of rodent whisking. I. Two-dimensional monitoring of whisker movements. Somatosens Mot Res 19:341–346.

Carvell GE, Simons DJ, Lichtenstein SH, Bryant P. 1991. Electromyographic activity of mystacial pad musculature during whisking behavior in the rat. Somatosens Mot Res 8:159–164.

Diogo R, Wood BA, Aziz MA, Burrows A. 2009. On the origin, homologies and evolution of primate facial muscles, with a particular focus on hominoids and a suggested unifying nomenclature for the facial muscles of the Mammalia. J Anat 215:300–319.

Dorfl J. 1982. The musculature of the mystacial vibrissae of the white mouse. J Anat 135:147–154.

Erzurumlu RS, Jhaveri S. 1992. Trigeminal ganglion cell processes are spatially ordered prior to the differentiation of the vibrissa pad. J Neurosci 12:3946–3955.

Erzurumlu RS, Killackey HP. 1983. Development of order in the rat trigeminal system. J Comp Neurol 213:365–380.

Gauthier GF. 1969. On the relationship of ultrastructural and cytochemical features to color in mammalia skeletal muscle. Z Zellforsch 95:462–482.

Gauthier GF, Dunn RA. 1973. Ultrastructural and cytochemical features of mammalian skeletal muscle fibers following denervation. J Cell Sci 12:525–547.

Grant RA, Mitchison B, Fox CW, Prescott TJ. 2009. Active touch sensing in the rat: anticipatory and regulatory control of whisker movements during surface exploration. J Neurophysiol 101: 862–874.

Guntinas-Lichius O, Irintchev A, Streppel M, Lenzen M, Grosheva M, Wewetzer K, Neiss WF, Angelov DN. 2005. Factors limiting motor recovery after facial nerve transection in the rat: combined structural and functional analyses. Eur J Neurosci 21:391–402.

Haidarliu S, Ahissar E. 1997. Spatial organization of facial vibrissae and cortical barrels in the guinea pig and golden hamster. J Comp Neurol 385:515–527.

Haidarliu S, Ahissar E. 2001. Size gradients of barreloids in the rat thalamus. J Comp Neurol 429, 372–387. Erratum in: J Comp Neurol 431:127–128.

Hill DN, Bermejo R, Zeigler HP, Kleinfeld D. 2008. Biomechanics of the vibrissa motor plant in rat: rhythmic whisking consists of triphasic neuromuscular activity. J Neurosci 28:3438–3455.

Huber E. 1930a. Evolution of facial musculature and cutaneous field of trigeminus. Part I. Quart Rev Biol 5:133–188.

Huber E. 1930b. Evolution of facial musculature and cutaneous field of trigeminus. Part II. Quart Rev Biol 5:389–437.

Jin T-E, Witzemann V, Brecht M. 2004. Fiber types of the intrinsic whisker muscle and whisking behavior. J Neurosci 24:3386–3393.

Klingener D. 1964. The comparative myology of four dipodoid rodents (Genera *Zapus, Napeozapus, Sicista,* and *Jaculus*). Misc Publ Mus Zool Univ Michigan 124:1–100.

Knutsen PM, Biess A, Ahissar E. 2008. Vibrissal kinematics in 3D: tight coupling of azimuth, elevation, and torsion across different whisking modes. Neuron 59:35–42.

Mitchinson B, Arabzadeh E, Diamond ME, Prescott TJ. 2008. Spike-timing in primary sensory neurons: a model of somatosensory transduction in the rat. Biol Cybern 98:185–194.

Nguyen Q-T, Kleinfeld D. 2005. Positive feedback in a brainstem tactile sensorimotor loop. Neuron 45:447–457.

Niederle B, Mayr R. 1978. Course of denervation atrophy in type I and type II fibers of rat extensor digitorum longus muscle. Anat Embriol 153:9–21.

Padykula HA, Gauthier GF. 1970. The ultrastructure of the neuromuscular junctions of mammalian red, white, and intermediate skeletal muscle fibers. J Cell Biol 46:27–41.

Pearson MJ, Pipe AG, Melhuish C, Mitchinson B, Prescott TJ. 2007. Whiskerbot: a robotic active touch system modeled on the rat whisker sensory system. Adapt Behav 15:223–240.

Rinker GC. 1954. The comparative myology of the mammalian genera *Sigmodon, Oryzomys, Neotoma,* and *Peromyscus* (Cricetinae), with remarks on their intergeneric relationships. Misc Publ Mus Zool Univ Michigan 83:1–25.

Ryan JM. 1989. Comparative myology and polygenetic systematics of the Heteromyidae (Mammalia, Rodentia). Misc Publ Mus Zool Univ Michigan 176:1–103.

Sachdev RN, Sato T, Ebner FF. 2002. Divergent movement of adjacent whiskers. J Neurophysiol 87:1440–1448.

Shaw F-Z, Liao Y-F. 2005. Relation between activities of the cortex and vibrissae muscles during high-voltage rhythmic spike discharges in rats. J Neurophysiol 93:2435–2448.

Terminologia Anatomica. 1998. Federative committee on anatomical terminology. Stuttgard: Georg Thieme.

Van Exan RJ, Hardy MH. 1980. A spatial relationship between innervation and the early differentiation of vibrissa follicles in the embrionic mouse. J Anat 131:643–656.

Vincent SB. 1912. The function of vibrissae in the behavior of the white rat. Behav Monog 1:1–81.

White KK, Vaughan DW. 1991. The effects of age on atrophy and recovery in denervated fiber types of the rat nasolabialis muscle. Anat Rec 229:149–158.

Whitmore I. 1999 Terminologia Anatomica: new terminology for the new anatomist. Anat Rec (New Anat) 257:50–53.

Wineski LE. 1985 Facial morphology and vibrissal movement in the golden hamster. J Morphol 183:199–217.

Wong-Riley M. 1979. Changes in the visual system of monocularly sutured or enucleated cats demostrable with cytochrome oxydase histochemistry. Brain Res 171:11–28.

Wrenn JT, Wessells NK. 1984. The early development of mystacial vibrissae in the mouse. J Embryol Exp Morph 83:137–156.

Yamakado M, Yohro T. 1979. Subdivision of mouse vibrissae on an embriological basis, with descriptions of variations in the number and arrangement of sinus hairs and cortical barrels in BALB/c (nu/+; nude, nu/nu) and hairless (hr/hr) strains. Am J Anat 155:153–174.